NASA/TM–20210013939

Development of a Numerical Modeling Approach for Buckling Analysis of Sandwich Composite Cylindrical Shells with Selected Results

Kyongchan Song, Arunkumar Satyanarayana, Adam Przekop, and Marc R. Schultz
Langley Research Center, Hampton, Virginia

April 2021

NASA STI Program Report Series

Since its founding, NASA has been dedicated to the advancement of aeronautics and space science. The NASA scientific and technical information (STI) program plays a key part in helping NASA maintain this important role.

The NASA STI program operates under the auspices of the Agency Chief Information Officer. It collects, organizes, provides for archiving, and disseminates NASA's STI. The NASA STI program provides access to the NTRS Registered and its public interface, the NASA Technical Reports Server, thus providing one of the largest collections of aeronautical and space science STI in the world. Results are published in both non-NASA channels and by NASA in the NASA STI Report Series, which includes the following report types:

- TECHNICAL PUBLICATION. Reports of completed research or a major significant phase of research that present the results of NASA Programs and include extensive data or theoretical analysis. Includes compilations of significant scientific and technical data and information deemed to be of continuing reference value. NASA counterpart of peer-reviewed formal professional papers but has less stringent limitations on manuscript length and extent of graphic presentations.

- TECHNICAL MEMORANDUM. Scientific and technical findings that are preliminary or of specialized interest, e.g., quick release reports, working papers, and bibliographies that contain minimal annotation. Does not contain extensive analysis.

- CONTRACTOR REPORT. Scientific and technical findings by NASA-sponsored contractors and grantees.

- CONFERENCE PUBLICATION. Collected papers from scientific and technical conferences, symposia, seminars, or other meetings sponsored or co-sponsored by NASA.

- SPECIAL PUBLICATION. Scientific, technical, or historical information from NASA programs, projects, and missions, often concerned with subjects having substantial public interest.

- TECHNICAL TRANSLATION. English-language translations of foreign scientific and technical material pertinent to NASA's mission.

Specialized services also include organizing and publishing research results, distributing specialized research announcements and feeds, providing information desk and personal search support, and enabling data exchange services.

For more information about the NASA STI program, see the following:

- Access the NASA STI program home page at http://www.sti.nasa.gov

- Help desk contact information:

https://www.sti.nasa.gov/sti-contact-form/
and select the "General" help request type.

NASA/TM–20210013939

Development of a Numerical Modeling Approach for Buckling Analysis of Sandwich Composite Cylindrical Shells with Selected Results

Kyongchan Song, Arunkumar Satyanarayana, Adam Przekop, and Marc R. Schultz
Langley Research Center, Hampton, Virginia

National Aeronautics and
Space Administration

Langley Research Center
Hampton, Virginia 23681-2199

April 2021

Available from:

NASA STI Program / Mail Stop 148
NASA Langley Research Center
Hampton, VA 23681-2199
Fax: 757-864-6500

Table of Contents

List of Figures

List of Tables

Nomenclature

α	Rayleigh mass proportional material damping factor
β	Rayleigh stiffness proportional material damping factor
ν_{12}	In-plane Poisson ratio
CID	User defined coordinate-system
D	Cylinder midsurface diameter
DOF	Degree of freedom
E_1, E_2	In-plane extensional moduli in the fiber and matrix directions, respectively
ξ	Damping coefficient
f	Natural frequency
FEA	Finite element analysis
FEM	Finite element model
G_{12}	In-plane shear modulus
G_{13}, G_{23}	Transverse shear moduli in the axial and circumferential directions, respectively
IML	Inner mold line
L	Cylinder length
MAP	Modeling and analysis plan
NESC	NASA Engineering and Safety Center
OML	Outer mold line
SBKF	Shell Buckling Knockdown Factor Project
t_c	Core thickness
t_f	Facesheet thickness

Abstract

The buckling response of geometrically perfect and imperfect cylindrical sandwich shells can be investigated using nonlinear finite element analyses with two-dimensional general-purpose shell elements. Such analyses are used in the NASA Engineering and Safety Center Shell Buckling Knockdown Factor Project, which has the goal of developing new analysis-based buckling design recommendations for select classes of sandwich composite cylindrical structures under uniaxial compressive load. As such, finite element models of sandwich composite cylinders were developed and analyses were performed to predict the buckling responses of geometrically perfect and imperfect sandwich composite cylinders. The development of the selected finite-element modeling approach for a sandwich composite cylinder is discussed. Buckling-response sensitivity of geometrically imperfect sandwich cylinders for various shell element types were investigated as part of this study. Preliminary results of geometric imperfections influence on buckling response of sandwich cylinders are also presented.

1.0 Introduction

The buckling response of thin shell structures can be very sensitive to imperfections. Generally, the most critical imperfections are geometric and loading imperfections. This imperfection sensitivity is generally addressed during design by applying a design factor (buckling knockdown factor) to the calculated classical linear buckling load of the perfect structure to reduce the calculated buckling load to a safe level. One of the goals of the NASA Engineering and Safety Center (NESC) Shell Buckling Knockdown Factor (SBKF) Project is to develop buckling design recommendations for a select class of composite launch-vehicle structures. As part of SBKF [1,2], finite element models (FEMs) of sandwich composite cylinders were developed and analyses were performed to predict the buckling responses of geometrically perfect and imperfect sandwich composite cylinders. When performing such analysis efforts, it is important to have a well-defined modeling and analysis plan (MAP), which provides guidelines in FEM development based on solid rational to ensure that each analysis is performed in the consistent decided-upon way [3,4,5]. The present document presents the developmental study undertaken to select the modeling approach. Several finite-element analysis (FEA) methods [6,7] were considered including linear buckling, and both nonlinear static and nonlinear transient analyses. Additionally, the modeling study discussed herein was focused on FEMs with two-dimensional general-purpose shell elements in a manner similar to that in Ref. [5], but modified for sandwich composite cylinders.

As the first step in the development of a FEM, the analyst has many factors to consider such as the element type, the element size, material property definition, and the methods for application of boundary and loading conditions. These factors were considered and studied as described below. Once developed, a FEM also needs to go through series of checks to verify that it complies with the selected approach.

The present report has two primary objectives. The first objective is to discuss the chosen analysis method, rationale, and procedures to predict buckling response of geometrically perfect and imperfect sandwich composite cylinders. The second objective is to provide results from selected

FEAs and characterize the system response and parameter sensitivities. For these purposes, the influence on the predicted buckling load of two-dimensional general-purpose shell element types and their size were studied. Based on this study, a preferred general-purpose shell element and element size was selected for the SBKF FEAs of sandwich composite cylinders.

In Section 2, the geometric description of the sandwich composite cylinders, the material system, and the modeling approach used in applying compressive load and boundary conditions to a sandwich composite cylinder are explained. In addition, various analysis types are discussed. In Section 3, results from the sensitivity analysis of geometrically perfect and imperfect sandwich composite cylinders are presented. In this section, the influence of different parameters including shell element types, size, and geometric imperfections on the buckling analysis of a sandwich composite cylinder are presented. A load plateau response was predicted for the perfect cylinder (no imperfection) models in the nonlinear buckling analyses. In Section 4, the predicted load plateau response of the perfect cylinder model is discussed. Finally, conclusions are given in Section 5. Typical example input decks for frequency extraction, bifurcation, nonlinear static, and transient dynamic analyses are presented in Appendix A. A check list to be used by an independent reviewer for model verification is also attached in Appendix B.

2.0 Modeling of Sandwich Composite Cylinders for Buckling Analysis

The purpose of the sandwich composite cylinder FEMs was to predict the buckling response of perfect and imperfect sandwich composite cylinders, and to study the influence of geometric imperfections on the buckling response. Geometric imperfections included in a FEM can be based upon the measured geometry of test articles or they can be assumed, e.g., defined analytically using eigenmode shapes or other perturbations. The general-purpose finite element software Abaqus/Standard 2016 [6] was used for this work. MSC Patran [7] and scripts within the framework of Patran were used in the development of FEMs and Abaqus/Viewer 2016 [6] was used for postprocessing of results.

The underlying sandwich composite cylinder design, the sources of input of the FEM, application of boundary conditions and loading, and analysis procedure are discussed in following sub-sections.

2.1 Geometry, Layup, and Material System

A 180-inch-long cylinder with a midsurface diameter of 331 inches was considered as is shown in Fig. 1. The cylindrical coordinate system with one axis aligned with the cylindrical axis of rotation and the origin in the plane of the bottom circumferential edge was used in this study and is shown in Fig. 2(a). The facesheet and core material orientations were defined in the shell section definition using the local coordinates where the 1-axis is the fiber orientation direction or the core ribbon direction and 3-axis is the normal direction, as shown in Fig. 2(b). The 0-degree fiber ply is aligned along the cylinder's axial axis.

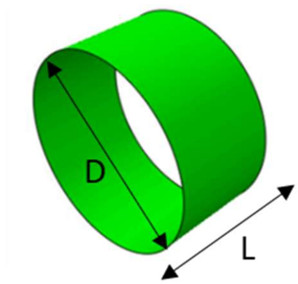

Figure 1. Sandwich composite cylinder with midsurface diameter, D, of 331 inch and length, L, of 180 inch.

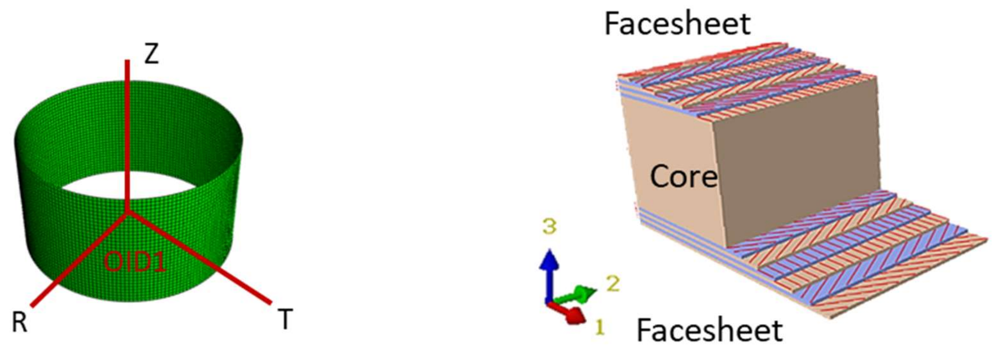

a) Global (cylindrical). b) Material orientation.

Figure 2. Coordinate systems.

Three facesheet layups were considered: quasi-isotropic and axially stiff layups made from IM7/8552 unidirectional tape plies, and a fabric layup consisting of IM7/8552 plain-weave fabric plies. The quasi-isotropic and axially stiff unidirectional tape layups had stacking sequences of $[\pm45/90/0]_S$ and $[+45/-45/90/0/0]_S$, respectively, and the fabric layup had a stacking sequence of $[+45/0/0/0/0/+45]_T$. The core material considered in this study was a Hexcel 3.1 pcf 1/8-5056-0.0007 aluminum honeycomb with various thicknesses. All materials were treated as linear elastic isotropic at room temperature. The material properties of the facesheet and core material systems are provided in Table 1.

Table 1. Material properties.

Properties	IM7/8552 unidirectional tape [8]	IM7/8552 fabric [9]	Aluminum honeycomb core Hexcel 3.1 pcf 1/8-5056-0.0007 [10]
Thickness (inch)†, t_f, t_c	0.0054	0.00787	0.5, 0.75, 1.0
E_1 (Msi)	20.04	10.585	0.001
E_2 (Msi)	1.33	10.586	0.001
G_{12} (Msi)	0.68	0.696	0.000345
G_{13} (Msi)	0.68	0.595	0.045
G_{23} (Msi)	0.408	0.595	0.020
ν_{12}	0.316	0.35	0.45

†Thickness values chosen for this study, note the given references.

The facesheets and core of the sandwich composite cylinder were discretized using two-dimensional general-purpose shell elements. Because general-purpose shell elements were used, the element membrane response was treated with a finite-strain formulation that gives accurate solutions to in-plane bending problems, is not sensitive to element distortion, and avoids parasitic locking [6]. For sandwich shell sections, the transverse shear stiffness values required in the element formulation were calculated by Abaqus. In the analyses, the core was treated as a linear elastic orthotropic continuum and only balanced and symmetric facesheets were considered. Since the cylinders considered here had a large diameter compared to the thickness, the effects of individual shell element curvature were neglected. In the finite element shell models, the midsurface coincided with the reference surface for the geometrically perfect models.

2.2 Application of Boundary and Load Conditions

Boundary conditions applied at the circumferential edges of the cylinder can influence the buckling response of the cylinder in significant ways. For example, clamped boundary conditions generally lead to a larger buckling load than simply supported boundary conditions. Simply supported boundary conditions were used at the circumferential edges of the cylinder in all analyses performed in this study. Specifically, with these conditions the nodes on the circumferential edges were allowed to rotate freely with respect to the tangent of the circumferential edge. For the applied compression, displacement was assumed to be uniform at top and bottom ends.

The boundary and load conditions were implemented by coupling nodes on the circumferential edge to a central reference node at each end, which lies in the end plane of the cylinder along the axis of rotation; the degrees of freedom (DOFs) of the reference node were defined by the cylindrical coordinate system. This node configuration was considered here as a *wagon-wheel* configuration and is shown in Fig. 3. All three translational displacements (U_R, U_θ, U_Z) and two rotational displacements (R_R and R_Z) between the center node and the nodes on circumferential edge were linked through the kinematic coupling command defined in the Abaqus input deck, which resulted in a simply supported shell edge. The center node at the bottom (origin) end was fixed in all DOFs and the center node at the top (positive Z) end was fixed in all DOFs except the axial displacement. An axial displacement was applied to this node as shown in Fig. 4.

Note that the user defined Coordinate-system (CID) of the coupling nodes must be used in the *KINEMATIC COUPLING card for proper coupling of DOFs between the center node and the nodes on the circumferential edge.

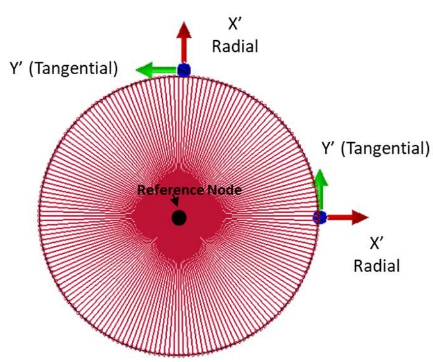

Figure 3. Kinematic coupling between center reference node and circumferential nodes.

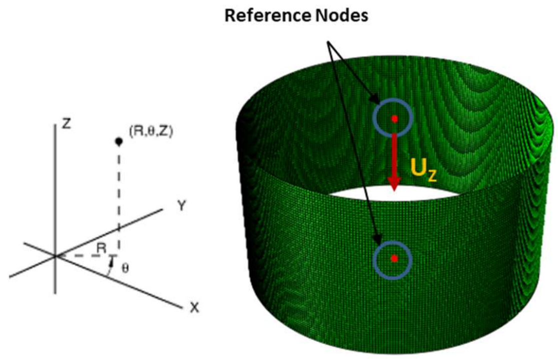

Figure 4. Boundary condition at center reference nodes in cylindrical coordinates.

2.3 Finite Element Analysis

To predict the buckling response of a sandwich composite cylinder, FEAs were performed utilizing four different analysis procedures: natural frequency, linear buckling, nonlinear static, and nonlinear transient dynamic analysis. Since the goal of the analysis efforts was to predict the buckling load and displacements of sandwich composite cylinders, strength failures of the facesheet, core, and the interface between facesheets and core were not considered.

Except as described below, the default FEA solution parameters such as solution convergence tolerance and numerical damping were used for all the analysis methods. While performing frequency analysis, and linear bifurcation (buckling) analysis, the built-in Lanczos solver was used to evaluate vibration or buckling load and modes.

The following load and analysis step parameters were used: for the static nonlinear analysis, the automated step-size adjustment was allowed with the minimum step size not less than 0.001 and maximum step not greater than 0.05 when the total analysis length was set to unity. In order to ensure quasistatic loading during the transient dynamic analyses, the load was applied in displacement control using constant-rate end shortening to 2.0 inches over a pseudo time of 1800 seconds. Solution parameter "halftol" was set approximately equal to the buckling load of the cylinder, and the default solution damping value of -0.05 was used in this study. Typical example input decks for frequency extraction, bifurcation, nonlinear static and transient dynamic analyses, are presented in Appendix A.

After the FEM was developed based on the analysis objectives, it was recommended that the FEM be checked by an independent reviewer. Therefore, a checklist of the FEM details and modeling parameters was generated and delivered to an independent reviewer to perform model verification based on a model check list which was similar to the one described in Ref [11]. By utilizing the model checklist, the reviewer can clearly understand the FEM input format, its purpose, and can identify potential mistakes made by the modeler as the first step of the review process. An example of the model checklist for a composite sandwich cylinder is included in Appendix B.

For each series of analyses, the first FEA performed was the frequency extraction analysis. The results from this frequency analysis were then used to determine the material damping factors for other analysis types as described in the next paragraph.

When performing dynamic analyses, it is important to use appropriate damping coefficients that are large enough to prevent unrealistic numerical vibrations, but small enough so that they will not suppress realistic behavior. Both, Rayleigh mass proportional (α) and Rayleigh stiffness proportional (β) damping are applied to the model during transient dynamic analysis. The process to calculate these damping factors is described in Ref. [12] and the damping factors are calculated using the equations

$$\alpha = 2\pi f\xi \qquad \beta = \frac{\xi}{2\pi f}$$

where f is the natural frequency of the finite element model and ξ is the damping coefficient. In this work, a damping coefficient, ξ, of 0.05 was used. Table 2 shows an example of these calculated damping factors for the sandwich composite cylinder shown in Fig. 1.

Table 2. Natural frequency and Damping Factors.

Sandwich Cylinder ID	Natural Frequency (Hz)	Damping Factors	
		α	β
SC-1	21.725	6.825	3.663×10^{-4}

3.0 Sensitivity Analysis of Perfect and Imperfect Buckling Response of Geometrically Perfect and Imperfect Sandwich Composite Cylinders

Sensitivity analysis of modeling parameters including shell element types, size, and geometric imperfections on the prediction of buckling response of a sandwich composite cylinder was performed to select the proper modeling parameters that ensure the design specifications and intended modeling assumptions of FEMs. In this section, results from the buckling analysis of a cylinder for several shell element types and sizes are presented. Then, the influence of shell element types on the buckling analysis of geometrically perfect and imperfect cylinders is presented. In addition, the influence of analysis convergence parameters of the geometrically perfect sandwich composite cylinder model is discussed. Based on the results of the sensitivity analysis, a shell element type and size were selected to develop subsequent FEMs for sandwich composite cylinders.

3.1 Finite Element Type and Mesh Convergence Study

For modeling a sandwich composite shell that contains a soft nonisotropic core material, the Abaqus *User's Guide* recommends using a general-purpose shell element or continuum shell elements [6]. The Abaqus general-purpose shell elements are S4, S4R, S4R5, S8R, and S8R5. The description of general-purpose shell elements and their integration points in first- and second-order shell elements are shown in Tables 3 and 4, respectively.

Table 3. General-purpose shell elements available in Abaqus.

Element	Description
S4	Four-node general-purpose shell, finite membrane strains
S4R	Four-node general-purpose shell, reduced integration with hourglass control, finite membrane strains
S4R5	Four-node thin shell, reduced integration with hourglass control, using 5 DOFs per node, no drilling DOF
S8R	Eight-node doubly curved thick shell, reduced integration
S8R5	Eight-node doubly curved thin shell, reduced integration, using 5 DOFs per node, no drilling DOF

Table 4. Integration points in Abaqus first- and second-order shell elements [6].

	Full integration	Reduced integration
First-order interpolation S4	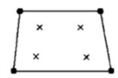	
Second-order interpolation S8	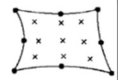	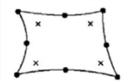

The purpose of this study was to obtain a converged mesh size for a sandwich composite cylinder subjected to a compression load for a given geometry definition, and to investigate the influence of the general-purpose shell-element type in Abaqus on the predicted buckling load and load-displacement response. Three different meshes were generated for the mesh convergence study of the180-inch-long cylinder:

- 0.5-degree mesh: 720 elements along circumference, 1.45-inch square element size
- 1.0-degree mesh: 360 elements along circumference, 2.90-inch square element size
- 2.0-degree mesh: 180 elements along circumference, 5.80-inch square element size

This study consisted of performing bifurcation buckling and nonlinear static buckling analyses. The default bifurcation buckling analysis solver in Abaqus is the subspace iteration eigensolver. However, the built-in Lanczos solver can also be used to calculate the linear buckling responses with less computing cost than the subspace iteration eigensolver. The bifurcation buckling analysis utilized the Lanczos solver with at least the lowest 10 eigenvalues requested.

Linear bifurcation buckling analyses were performed on FEMs of a cylinder with quasi-isotropic facesheets and a 0.5-inch-thick core to investigate the influence of shell element type and mesh size on the predicted buckling load and modes. The lowest predicted buckling loads from the linear buckling analysis of FEMs are listed in Table 5. The variation of the buckling load with the shell element types considered in this study was negligible (with buckling loads well within 1% of each other) for the 0.5-degree and 1.0-degree meshes. The predicted buckling loads from the 2.0-degree mesh do not agree as well, with differences up to more than 3% from the 0.5-degree mesh. Therefore, only the 0.5-degree and 1.0-degree meshes with S4R element, i.e., meshes and elements with least computational cost (as measured by the number of integration points shown in Table 4), were considered for nonlinear static buckling analyses in the mesh convergence study.

Table 5. Predicted linear buckling loads (in lbf) as a function of element type and size.

	Abaqus Element Type				
Mesh	S4	S4R	S4R5	S8	S8R5
0.5 degree	2.325 E+6	2.325 E+6	2.325 E+6	2.330 E+6	2.326 E+6
1.0 degree	2.341 E+6	2.335 E+6	2.335 E+6	2.331 E+6	2.327 E+6
2.0 degree	2.403 E+6	2.332 E+6	2.332 E+6	2.341 E+6	2.329 E+6

Nonlinear static analyses were performed on FEMs of a sandwich composite cylinder for three facesheet stacking sequences and two core thicknesses (0.5 inch and 1.0 inch) as part of the mesh convergence study. Linear buckling and nonlinear peak loads are shown in Figs. 5 through 7 for quasi-isotropic, axially stiff, and fabric layups, respectively.

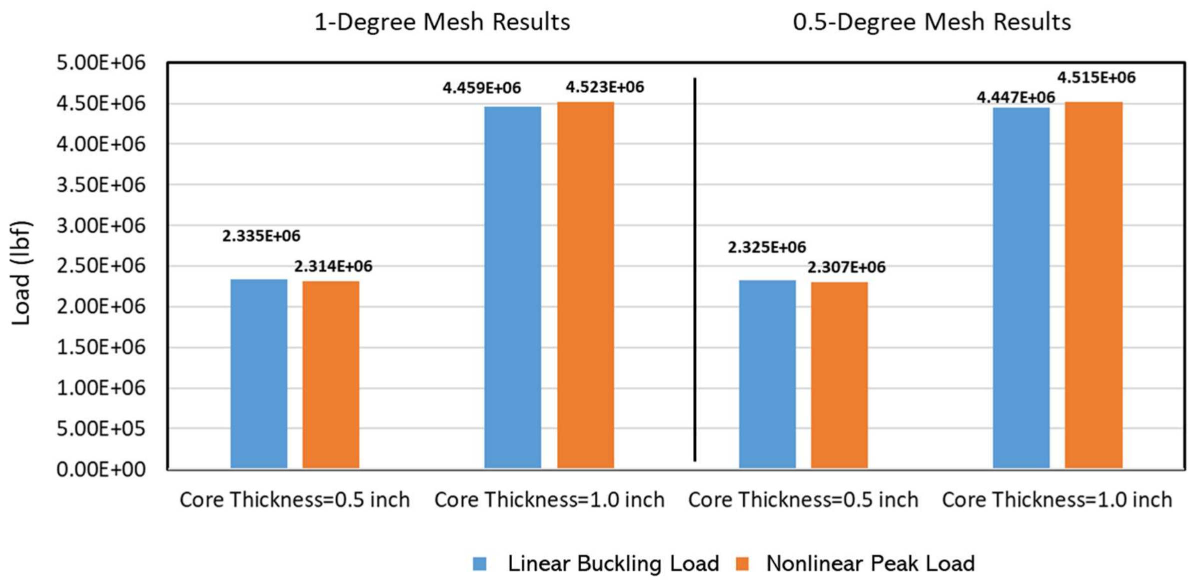

Figure 5. Linear buckling and nonlinear peak loads of FEM with quasi-isotropic facesheets.

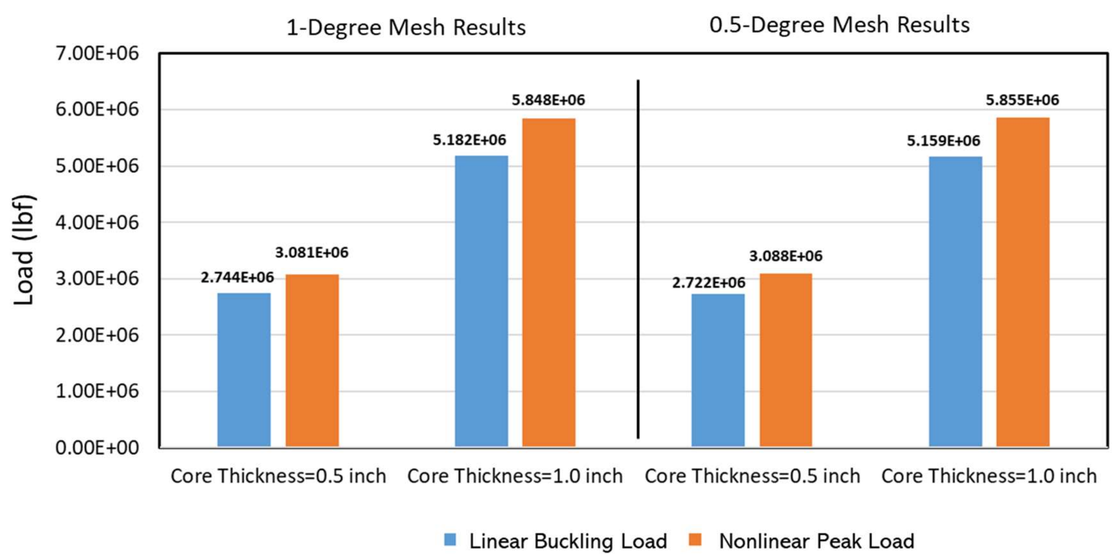

Figure 6. Linear buckling and nonlinear peak loads of FEM with axially stiff facesheets.

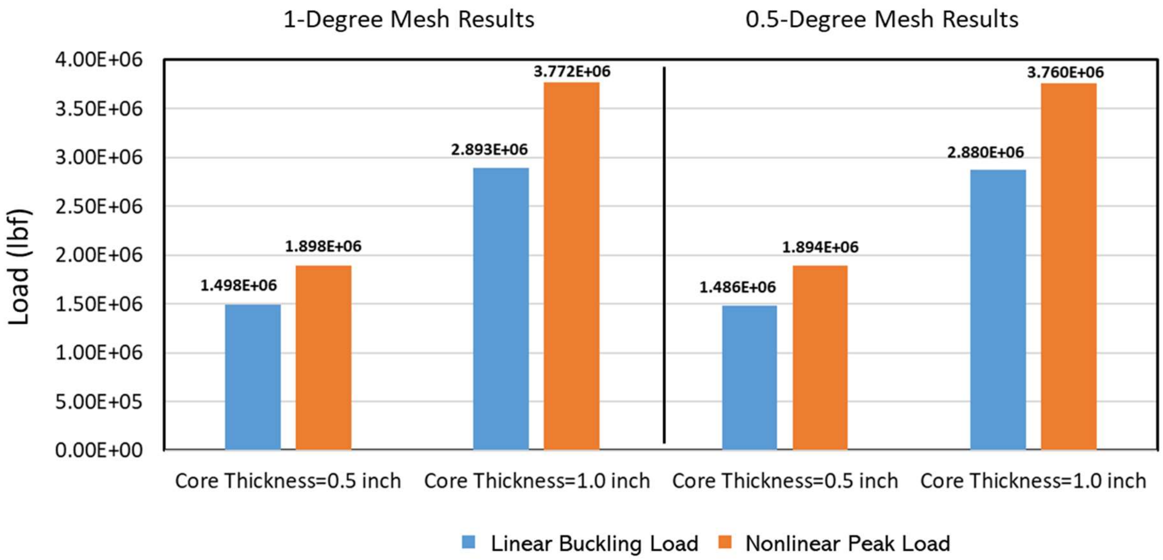

Figure 7. Linear buckling and nonlinear peak loads of FEM with fabric facesheets.

The linear buckling and peak load results presented in Figs. 5 through 7 indicate that the 1.0-degree mesh model which has 360 elements along circumference was a sufficiently refined model because corresponding results between the 0.5-degree mesh and the 1.0-degree mesh all agree within 1% for three varying facesheet layups and two different core thicknesses. Also, as shown in Fig. 8, both meshes show identical radial and axial displacement at the nonlinear peak load.

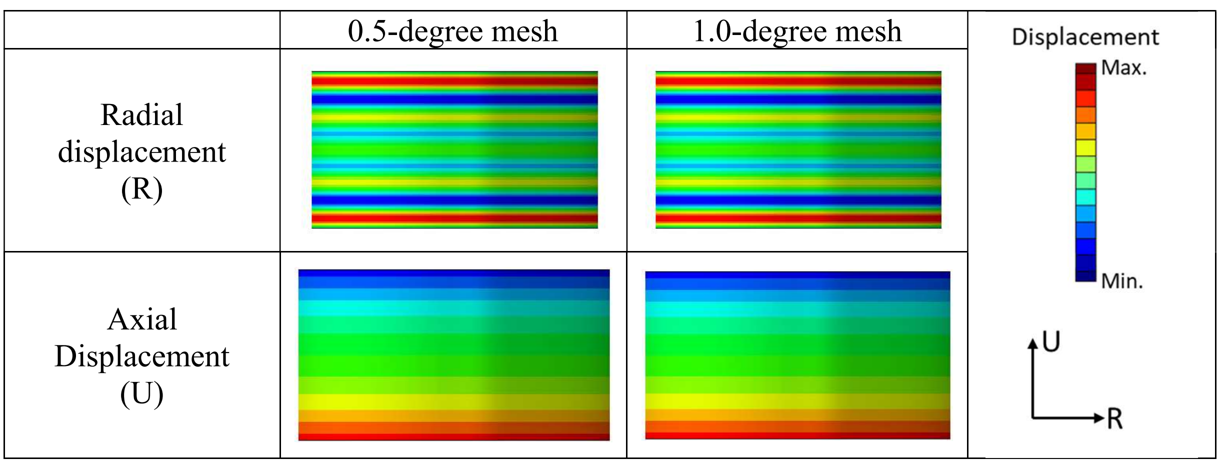

Figure 8. Radial and axial displacement contour plots of 0.5-degree and 1.0-degree mesh.

Based on these results, FEMs for more extensive parametric studies of the buckling response of sandwich composite cylinders were developed with different types of 2-dimensional general-purpose shell elements and the 1.0-degree mesh density along the circumferential direction.

3.2 Finite Element Type and Imperfection Sensitivity Analysis

The buckling loads and modes of sandwich composite cylinders are sensitive to imperfections in the geometry, thickness, and loading. In this regard, different modeling approaches can be used to impose geometric imperfections on a FEM. The midsurface geometric imperfection of the first SBKF 8-ft-diameter cylindrical composite test article (designated CTA8.1) is presented in Fig. 9 and was obtained by measuring the IML and the OML cylinder surfaces and averaging the two measurements [13]. This midsurface imperfection was scaled from its original length and diameter to fit the geometry of the present sandwich composite cylinders and was applied as a midsurface imperfection to the present FEMs using a special-purpose Python script "PyTiger" [14]. Imperfection sensitivity analysis was carried out to investigate the influence of the general-purpose shell element types on the predicted peak load and postbuckling response of geometrically imperfect sandwich composite cylinder models of a quasi-isotropic facesheet with a 1.0-inch-thick core. Transient dynamic analysis was performed on FEMs with 1.0-degree mesh, for different shell element types and four different amplitudes of the CTA8.1 geometric imperfection (no imperfection or geometrically perfect, 0.4-inch, 1.0-inch, and 2.0-inch peak-to-peak scaled imperfections). Predicted linear buckling and nonlinear peak loads obtained from linear bifurcation buckling and transient dynamic analyses are presented in Table 6.

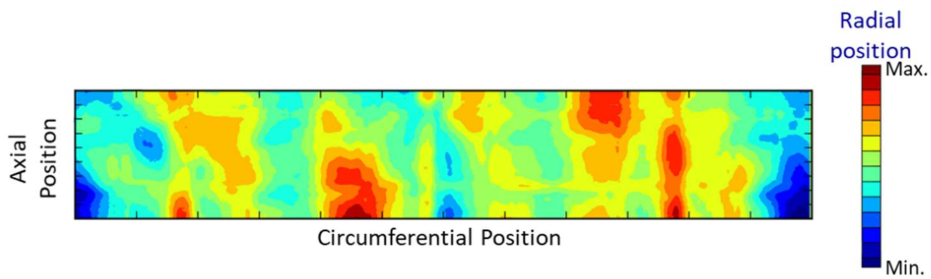

Figure 9. CTA8.1 test article midsurface geometric imperfection input.

Table 6. Predicted linear buckling and nonlinear peak loads (in lbf) for each element type for transient dynamic analysis.

	Abaqus Element Type				
Peak-to-peak imperfection	S4	S4R	S4R5	S8R	S8R5
Perfect (Linear Buckling)	4.464E+06	4.461E+06	4.437E+06	4.443E+06	4.439E+06
Perfect	4.540E+06	4.524E+06	4.421E+06	4.237E+06	4.371E+06
0.4 inch	3.739E+06	3.734E+06	3.698E+06	3.723E+06	3.715E+06
1.0 inch	3.374E+06	3.374E+06	3.336E+06	3.346E+06	3.343E+06
2.0 inch	2.870E+06	2.870E+06	2.837E+06	2.834E+06	2.698E+06

The results shown in Table 6 show some inconsistency in the predicted peak loads of the perfect shell when different shell element types are used. The predicted load versus end shortening curves of FEMs with the geometrically perfect 1.0-degree mesh using the different shell element types are presented in Fig. 10.

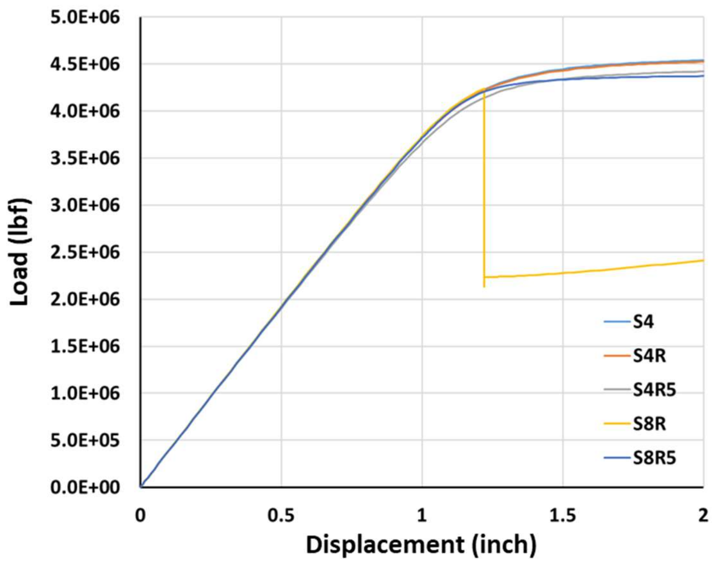

Figure 10. The predicted load versus end shortening curves of FEM for geometrically perfect shell.

As shown in Fig. 10, the peak load and postbuckling response of shell with S8R elements are different than the responses predicted with other shell elements. Specifically, the response predicted with the S8R elements is initially linear with nonlinearity occurring just before the load drop, and then a sudden load drop following the peak load. The predicted response for the remaining elements (S4, S4R, S4R5, and S8R5) are initially similar to that of the S8R elements, but show a flattening of the curve at the nonlinearity and the formation of a *load plateau* (characterized by little change in the load with continued end shortening) rather than the sudden load drop. In all cases observed, the load plateau was associated with extensive nonlinear growth of axisymmetric radial deformations with continued end shortening, and the load drop predicted with the S8R elements was associated with a breakdown of this axisymmetry. In contrast to the predicted responses of the perfect shell, neither the knee in the load versus end shortening curves or the extensive nonlinear growth of axisymmetric radial deformations were seen when geometric imperfections were included. Rather, the predicted responses were essentially linear until a sudden load drop occurred that was associated with a nonaxisymmetric deformation. The predicted peak load and postbuckling responses for the cylinder with geometric imperfections are all very similar for the different element types. The peak loads and postbuckling responses of the FEMs with the 0.4-inch peak-to-peak amplitude of CTA8.1 imperfection are shown in Fig. 11. The predicted peak loads and subsequent load drops are all very similar, however, the eight-noded elements (S8R and S8R5) show unstable responses and convergence problems after the load drop that lead to early termination of these analyses. These unstable responses and convergence problems are more apparent and occur earlier in the displacement for the 2.0-inch peak-to-peak imperfection as presented in Fig. 12. Additionally, the predicted response for the 2.0-inch peak-to-peak imperfection using S8R5 elements showed a larger load drop at about 0.7-inch displacement and the analysis terminated earlier than the predictions using the other element types.

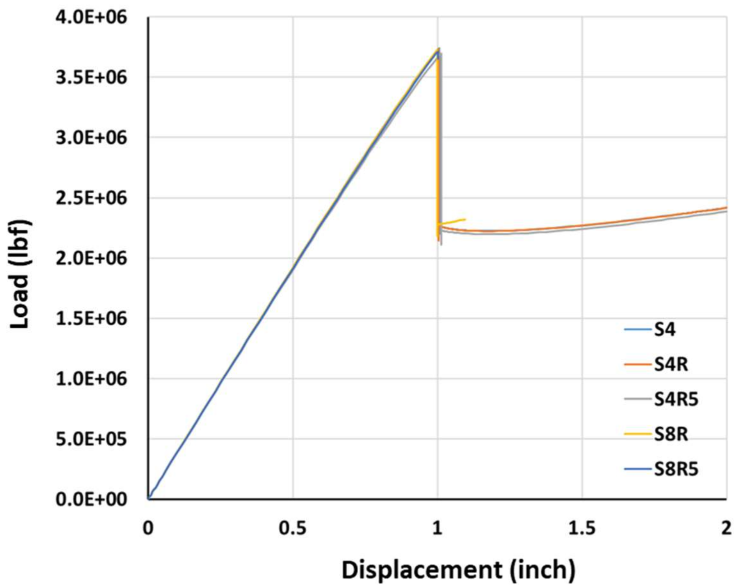

Figure 11. The predicted load versus end shortening curves of FEM with 0.4-inch peak-to-peak CTA8.1 imperfection.

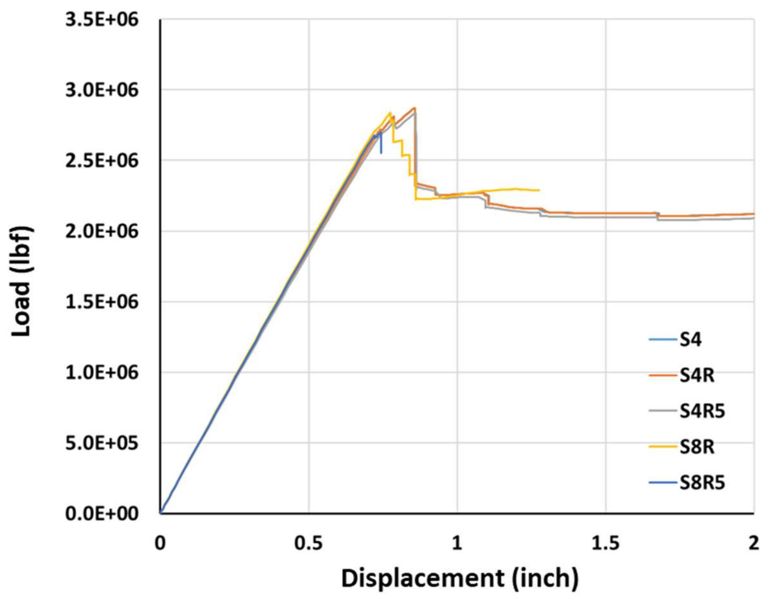

Figure 12. The predicted load versus end shortening curves of FEM with 2.0-inch peak-to-peak CTA8.1 imperfection.

Considering the postbuckling response, modeling effort, and the computational time, the four-noded, reduced integration with hourglass control, finite membrane strain, the general-purpose shell element, S4R, was chosen for discretizing the FEM of sandwich composite cylinder models.

3.3 Shell Element Selection

The buckling response of a sandwich composite cylinder under uniaxial compressive loading was studied here by structural shell analysis. The influence of two-dimensional general-purpose elements (S4, S4R, S4R5, S8R, S8R5) and its size (angular distance of 0.5 degree, 1.0 degree, and

2.0 degree) on the buckling load was investigated. Buckling load variation among the element types is less than 0.2% for an element size of 0.5 degree and a core thickness of 0.5 inch. A similar trend is noticed for other element sizes as well. A maximum variation in buckling load of 2.3% is noticed for S4 element type between the considered element sizes. Also, the influence of geometric imperfection of various magnitudes on buckling behavior of a sandwich cylinder constructed with several element types discussed earlier was investigated. The variation in buckling load for a 2.0-inch imperfection among element types is within 6%. Lowest buckling load of 2.698E+6 lbf, is obtained using the S8R5 element and a load of 2.87E+6 lbf is obtained for using the S4 element. However, for other imperfection magnitudes, the variation in buckling load among element types is within 1.2%. The peak load of the perfect cylinder with a 1.0-inch core thickness varies by 7% for the considered element types, but this variation is primarily due to the load plateau and presence or absence of a load drop as shown in Fig. 10. Based on these results, the S4R element with 1.0-degree circumferential angular length was selected because it was believed to be sufficient to develop sandwich composite cylinder models for the size and class of cylinders considered in this study, and to provide accurate buckling response prediction for an uniaxial compressive load condition.

4.0 Predicted Load Plateau Response of the Perfect-Mesh Cylinder Model

Nonlinear static analysis, which uses Newton's method, and nonlinear transient dynamic analysis, which uses direct integration, were performed to simulate prebuckling, buckling, and postbuckling response of the perfect sandwich composite cylinder. The transient dynamic analysis has the advantage that it is more likely to obtain a converged solution of the postbuckled cylinder. With small time increments, a transient dynamic analysis can solve nonlinear equilibrium equations with minimum vibrational response of the structure and numerical energy dissipation from the prebuckling configuration to a postbuckled equilibrium shape. For this reason, buckling analyses of sandwich composite cylinders are often conducted by the transient dynamic analysis to predict the postbuckled response of the sandwich composite cylinders.

A perfect cylinder model of the 120-inch-long and 96-inch-diameter cylinder with $[60/\text{-}60/0/0/\text{-}60/60]_T$ facesheet and a 0.2-inch-thick core was developed and buckling responses of the FEM were obtained by nonlinear static and nonlinear transient dynamic analyses. The predicted load versus end-shortening curves of the perfect-mesh model from these analyses are shown in Fig. 13. In this figure, it is seen that predictions from both the nonlinear static and transient dynamic analyses show the development of an extensive load plateau in the proximity of the buckling load. (Because the Abaqus solvers by default do not accept negative roots in the stiffness matrix, the equilibrium configurations in these plateau regions are predicted to be stable.). The predicted load-displacement response from the nonlinear static analysis has the load plateau continuing to the prescribed end displacement of 0.8 inch. However, the predicted load versus end-shortening curve from the transient dynamic analysis has the load plateau developing initially, but then a sudden load drop is predicted to occur at an end displacement of approximately 0.75 inch. The radial deformations of the cylinder at three different end-shortening levels, 0.6 inch, 0.75 inch, and the end of analyses, are presented in Fig. 14. It is seen that during the load plateau region of the load versus end-shortening curve, the predicted responses of both analyses are initially a stable axisymmetric deformation along the length. However, as the load drop is approached in the transient dynamic analysis, the axisymmetric response transitions to more localized inward dimples that grow in magnitude and eventually become unstable, at which point, the load drops.

Both analyses were repeated with the smaller step increments, but the predicted responses of the perfect-mesh model did not change appreciably.

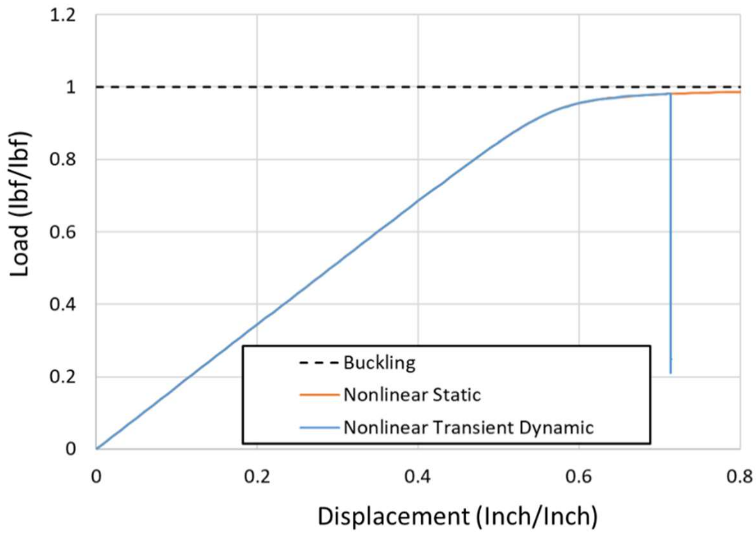

Figure 13. The predicted load versus end-shortening curves of perfect mesh-model with different analyses (applied load normalized to unity).

End Shorting	Nonlinear Static	Nonlinear Transient Dynamic	
at 0.6 inch	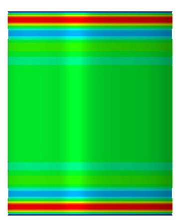	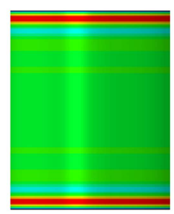	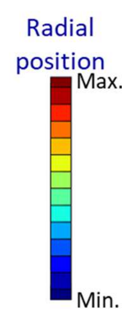
at 0.75 inch	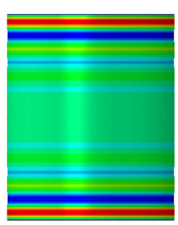	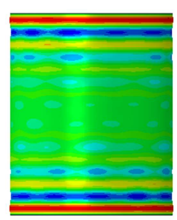	
at the end of analysis	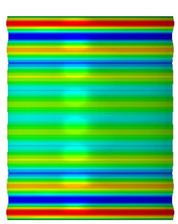	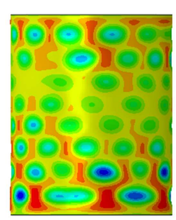	

Figure 14. Predicted radial displacements using the finite-element perfect-mesh model with nonlinear static and nonlinear transient dynamic analyses.

Further investigation of predicted load plateau response of the perfect cylinder model was performed and it was found that near the dynamic load-drop event in nonlinear static and nonlinear transient dynamic analyses of the perfect cylinder, the solution of nonlinear equilibrium equations depends not only on the step increment size but also on artificial solution damping and the convergence tolerance within a different analysis method. A total of 52 convergence parameters (29 force and moment convergence and 23 time incrementation parameters), are available in Abaqus to modify the convergence criteria and to obtain converged solutions when performing nonlinear static and transient dynamic analyses. The chosen tolerance values likely influence the predicted length of the load plateau past the knee in the load versus end shortening curve. However, for all the nonlinear analyses described herein, the default convergence tolerance parameters of nonlinear static and transient dynamic analysis were used. Additionally, the loading plateau was only seen when an axisymmetric buckling response was predicted, and this is likely an unrealistic response that would not have been seen in physical shells of the class of cylinders considered in this study because small geometric (as shown), loading, or other imperfections can lead to a nonaxisymmetric response that does not show the plateau behavior. If this plateau behavior is predicted during part of a design effort, the designer should consider interrogating the sensitivity of the plateau behavior to geometric or other imperfections, and may want to consider using the knee in the load versus end-shortening curve as the buckling load in a way similar to the way buckling is often classified for structures with a stable postbuckling response like beams, plates, or shallow-shells. Although both the transient dynamic analysis and nonlinear static analysis solutions were considered, the nonlinear transient dynamic analysis was selected for subsequent analyses within the SBKF Project becuase of the reduced computational cost and the ability to predict the postbuckled response of the considered sandwich composite cylinders.

5.0 Concluding Remarks

This report contains a discussion of the selection of the modeling approach adopted for developing finite element models (FEMs) of sandwich composite cylinders for buckling analyses for the NASA Engineering and Safety Center Shell Buckling Knockdown Factor Project. Modeling assumptions and approaches of FEMs to predict the buckling response of a sandwich composite cylinder were explained. Linear buckling, nonlinear static, and transient dynamic analyses were performed for geometrically perfect and imperfect sandwich composite cylinders using different types of shell elements to predict the buckling response. The results of a sensitivity analysis of the buckling response to element type and size show that S4R element of 1.0-degree angular length should be sufficient to develop sandwich composite cylinders of the size and class considered in this study.

The results of nonlinear static and transient dynamic analysis of the perfect mesh indicate that nonlinear analysis convergence parameters influence the predicted postbuckling response of the sandwich composite cylinder models. Even though converged solutions were obtained using nonlinear static or transient dynamic analysis, postbuckled response, specifically the length of a load plateau in the load versus end-shortening curve, was found to be influenced by the chosen solver convergence and damping parameters. Based on the study described herein, the nonlinear transient solver was chosen for continued analysis of the buckling response of sandwich composite cylindrical shells because of its ability to obtain a realistic converged solution for the postbuckled response of the sandwich composite cylinder model with imperfection and its usage of efficient computing resources.

6.0 References

[1] Hilburger, M.W., “Developing the Next Generation Shell Buckling Design Factors and Technologies,” 53rd AIAA/ASME/ASCE/AHS/ASC Structures, Structural Dynamics and Materials Conference, AIAA Paper 2012-1686, Honolulu, HI, April 2012.

[2] Schultz, M.R., Sleight, D.L., Myers, D.E., Waters, W.A. Jr., Chunchu, P.B., Lovejoy, A.E., and Hilburger, M.W., “Buckling Design and Imperfection Sensitivity of Sandwich Composite Launch-Vehicle Shell Structures,” Proceedings of the American Society for Composites: Thirty-First Technical Conference, Williamsburg, Virginia, September 19–21, 2016. DEStech Publications, Inc., CD-ROM.

[3] Knight, N.F., Nemeth, M.P., and Hilburger, M.W., “Assessment of Technologies for the Space Shuttle External Tank Thermal Protection System and Recommendations for Technology Improvement,” NASA TM-2004-213256, 2004.

[4] Lovejoy, A.E., and Hilburger, M.W., “SBKF Modeling and Analysis Plan: Buckling Analysis of Compression-Loaded Orthogrid and Isogrid Cylinders,” NASA TM-2013-218037, 2013.

[5] Adam E. Stockwell, “A Verification Procedure for MSC/NASTRAN Finite Element Models,” NASA CR- 4675, Hampton VA, June 1995.

[6] Anon., ABAQUS™ 2016 Analysis User's Guide, Vols. I-V, Version 2016. Dassault Systèmes, Providence, RI, 2016.

[7] Patran User’s Manual, Version 2014, MSC Software Corporation, 4675 MacArthur Court, Suite 900, Newport Beach, CA 92660.

[8] Marlett, K., Ng, Y., and Tomblin, J., “Hexcel 8552 IM7 Unidirectional Prepreg 190 gsm & 35% RC Qualification Material Property Data Report”, CAM-RP-2009-015 Rev A, April 23, 2011 report for IM7/8552 Unidirectional tape.

[9] Krueger, R., and Ratcliffe, J., “Analysis of Composite Panel-Stiffener Debonding Using a Shell/3D Modeling Technique,” NASA/CR-2007-214879, NIA Report No. 2007-07, June, 2007.

[10] Anon., “HexWeb Honeycomb Attributes and Properties,” Hexcel Composites, TSB 120, Pleasanton, CA, November 1999.

[11] Fowler, B. EV31-OWI-001 Revision C, “Organization Work Instruction EV31 Dynamics, Loads, And Strength Branch Structural Dynamics, Load and Strength Analysis”, Marshall Space Flight Center, 2017

[12] Knight, N.F, and Rankin, C.C, “STAGS Example Problems Manual,” NASA CR-2006-2144281, March, 2006.

[13] Schultz, M.R., Sleight, D.L., Gardner, N.W., Rudd, M.T., Hilburger, M.W., Palm, T.E., and Oldfield, N.J., “Test and Analysis of a Buckling-Critical Large-Scale Sandwich Composite Cylinder,” 58th AIAA/ASME/ASCE/AHS/ASC Structures, Structural Dynamics & Materials Conference, AIAA Paper 2018-1693, Orlando, FL, January 2018.

[14] Kosztowny, C.J., “Implementing Geometric Surface Imperfections into Sandwich Composite Cylinder Finite Element Method Models,” AIAA SciTech 2021 Forum, AIAA Paper 2021-0439, Virtual Event, January 2021.

Appendix A. Input example of a sandwich-composite cylinder

Frequency Extraction Analysis Input Deck:

```
*HEADING
ABAQUS job created on 12-Mar-13 at 16:45:17
**
*NODE
      1,      -163.56,     -2.58956,      75.4985
      2,      -163.56,     -2.58956,       74.492
      3,      -163.56,     -2.58956,      73.4855
      4,      -163.56,     -2.58956,       72.479
       .
       .
  415889,           0.,           0.
  415891,           0.,           0.,      265.742
**
*TRANSFORM, TYPE=C, NSET=CID1
         0.,         0.,         0.,         0.,         0.,         1.
**
*NSET, NSET=CID1
  415889,   415891
**
*ELEMENT, TYPE=S4R5, ELSET=PR-SKIN
      1,  394501,  394502,  395375,  395374
      2,  394502,  394504,  395378,  395375
**
*SHELL SECTION, ELSET=PR-SKIN, MATERIAL=AL-2219
       0.19,      3
**
** al-2219
** Date: 12-Mar-13          Time: 16:32:02
**
*MATERIAL, NAME=AL-2219
**
*DENSITY
     0.000267,
**
*ELASTIC, TYPE=ISO
    1.05E+7,       0.33
**
*NSET, NSET=DISPL
415891
**
*NSET, NSET=FIXED
415889
**
*NSET, NSET=CID1
FIXED-NODES
DISPL-NODES
**
*KINEMATIC COUPLING, REF NODE=DISPL, ORIENTATION=CID1
DISPL-NODES     ,1,4
DISPL-NODES     ,6,6
*KINEMATIC COUPLING, REF NODE=FIXED, ORIENTATION=CID1
FIXED-NODES     ,1,4
```

```
FIXED-NODES     ,6,6
**
*STEP
Linear Static Analysis
**
This load case is the default load case that always appears
*FREQUENCY, EIGENSOLVER=LANCZOS
      10,   ,    ,    ,   ,
**
*BOUNDARY, OP=NEW
FIXED, 1,6,         0.
DISPL,1,2, 0.
DISPL,4,6, 0.
**
** NODE OUTPUT REQUESTS
**
*OUTPUT, FIELD, FREQ=1
*NODE OUTPUT
U,
**
*END STEP
```

Eigen Value Analysis Input Deck:

The model, node, element, material, shell-section and boundary conditions information is same as the one shown in frequency extraction analysis input deck above, except STEP info. The Step info is shown below.

```
*STEP
*BUCKLE, EIGENSOLVER=LANCZOS
10, , , ,
**
*CLOAD, OP=MOD
DISPL, 3,        -1.0
**
*BOUNDARY, OP=MOD
FIXED, 1,6,         0.
DISPL, 1,2,         0.
DISPL, 4,6,         0.
**
*OUTPUT, FIELD, FREQ=1
*NODE OUTPUT
U,
**
*END STEP
```

Non-Linear Static Analysis Input Deck:

The model, node, element, material, shell-section and boundary conditions information is same as the one shown in frequency extraction analysis input deck above, except STEP info. The Step info is shown below.

```
*STEP, NLGEOM=YES, INC=100
*STATIC
0.05, 1.0, 0.001, 0.05
**
*BOUNDARY, OP=MOD
FIXED, 1,6,         0.
DISPL, 1,2,         0.
DISPL, 3,,        -0.1
DISPL, 4,6,         0.
**
*OUTPUT, FIELD, FREQ=1
*NODE OUTPUT
```

```
U,
*NODE OUTPUT, NSET=FIXED
RF,
**
*END STEP
```

Non Linear Transient Dynamic Analysis Input Deck:

The model, node, element, material, shell-section and boundary conditions information is same as the one shown in frequency extraction analysis input deck above, except STEP info. The Step info is shown below.

```
**
*MATERIAL, NAME=AL-2219
**
*Damping, alpha=6.825, beta=0.0003663
**
*DENSITY
   0.000266,
**
*ELASTIC, TYPE=ISO
    1.05E+7,        0.33
**
*STEP,  INC=350, NLGEOM
**
*DYNAMIC, alpha=-0.05, haftol=1.0E+6
1.0, 1800.0, 0.0005, 20.0
**
*AMPLITUDE, NAME=RAMPA
0.0, 0.0, 1800.0, -1.0
**
*BOUNDARY, OP=MOD
FIXED, 1,6,          0.
DISPL, 1,2,          0.
DISPL, 4,6,          0.
**
*BOUNDARY, OP=MOD, AMPLITUDE=RAMPA
DISPL, 3, ,        1.0
**
** NODE OUTPUT REQUESTS
**
*OUTPUT, FIELD, FREQ=1
*NODE OUTPUT
U,
*NODE OUTPUT, NSET=FIXED
RF,
**
** ELEMENT OUTPUT REQUESTS
**
*OUTPUT, FIELD, FREQ=10
**
*ELEMENT OUTPUT, POS=INTEG, ELSET=BARL5-PANEL-WELDLAND
1, 2,3,4,5,6,7,8,9,10,11,12,13,14,15,16
S,
E,
**
*END STEP
```

Appendix B. Model check list

Date :								
Model Name:	Model Revision/Version :							
Reviewer :								
brief description of Model : This is an example of quasi-isotropic facesheet nominal model check list								
Geometric & Mesh Data Checks	**Reference**							**Check**
Imperfection								Norminal
Check coordinate system use and definition								No
RBE (Boundary condition coordination)	0 degree							No
OID1 (Global material coordination)	90 Degree							No
Verify proper use of element types	S4R							No
Verify duplicate elements exist only as intended								No
Verify no unused nodes exist within model								No
Verify free edge definition								No
Material Data Checks								
	E	nu					Density	
Al6061-T6 property	1.02E+07	0.33					2.55E-04	No
	E1	E2	nu12	G12	G13	G23	Density	
Grout property	1.10E+03	1.10E+06	0.03	5.34E+05	5.34E+05	5.34E+05	1.55E-04	No
Facesheet property	2.04E+07	1.33E+06	3.45E-01	6.80E+05	6.80E+05	3.30E+05	1.48E-04	No
3p1 core property	5.8	2.9	0.8	1.45	45000	20000	4.65E-06	No
	XT	XC	YT	YC	S(Shear)			
Failure Index	3.55E+05	2.29E+05	1.55E+04	3.43E+04	1.42E+04			No
Shell Section Check								
	lamina	Core	IML AL	IML Grout	OML Grout	OML AL		
Thickness	0.00694	0.2	0.4	0.159	0.3022	0.5		No
Off from mid surface (-0.5 ~ 0.5)	0	0	0	0	0	0		No
Material orientation	OID1							No
Verify composite definition								
	Core Type	Layup						
Facesheet layout	8p1	[AL/GR/(60/-45/-60/45/0/)s]						No
PADUPBOT1	8p1	[60/-45/-60/45/0/]s						No
Boundary Condition Checks								
Check kinematic coupling definition								No
Verify the top reference node boundary condition	Tx,Ty,Rx,Ry,Rz=0.							No
Verify the bottom reference node boundary condition	Tx,Ty,Tz,Rx,Ry,Rz=0.							No
Dynamic Analysis Checks								
Check analysis type	Static Dynamic							No
Check time-dependant properties								No
Check Alpha damping factor	-0.333							No
Check HAFTOL	2.28E+06							No
Check history output request	Top_CRT_NODE (U,UF,RF)							No
Check field output request	S, E, Failure							No
Check amplitude								No
Results Checks								
Check for errors and warnings in the output								No
Verify that reaction force equals the applied force								No
Check the peak load								No
Additional Comments								

REPORT DOCUMENTATION PAGE	*Form Approved* *OMB No. 0704-0188*

1. REPORT DATE *(DD-MM-YYYY)*
01/04/2021

2. REPORT TYPE
TECHNICAL MEMORANDUM

3. DATES COVERED *(From - To)*
07/01/2015 - 4/20/2021

4. TITLE AND SUBTITLE
Development of a Numerical Modeling Approach for Buckling Analysis of Sandwich Composite Cylindrical Shells with Selected Results

5a. CONTRACT NUMBER

5b. GRANT NUMBER

5c. PROGRAM ELEMENT NUMBER

6. AUTHOR(S)
Song, Kyongchan; Satyanarayana, Arunkumar; Przekop, Adam;
Schultz, Marc R.;

5d. PROJECT NUMBER

5e. TASK NUMBER

5f. WORK UNIT NUMBER
869021.04.23.01.13

7. PERFORMING ORGANIZATION NAME(S) AND ADDRESS(ES)
NASA Langley Research Center
Hampton, VA 23681-2199

8. PERFORMING ORGANIZATION REPORT NUMBER

9. SPONSORING/MONITORING AGENCY NAME(S) AND ADDRESS(ES)
National Aeronautics and Space Administration
Washington, DC 20546-001

10. SPONSOR/MONITOR'S ACRONYM(S)
NASA

11. SPONSOR/MONITOR'S REPORT NUMBER(S)
NASA/TM-20210013939

12. DISTRIBUTION/AVAILABILITY STATEMENT
Unclassified - Unlimited
Subject Category
Availability: NASA STI Program (757) 864-9658

13. SUPPLEMENTARY NOTES

14. ABSTRACT
The buckling response of geometrically perfect and imperfect cylindrical sandwich shells can be investigated using nonlinear finite element analyses with two-dimensional general-purpose shell elements. The development of a finite- element modeling approach to predict the buckling response of sandwich composite cylinders is discussed. This modeling approach was used to investigate the buckling-response sensitivity of geometrically imperfect sandwich cylinders for various shell element types. Preliminary results of the influence of geometric imperfections on the buckling response of sandwich cylinders are also presented.

15. SUBJECT TERMS
Sandwich composite cylinders; buckling; finite element analysis; finite element modeling

16. SECURITY CLASSIFICATION OF: a. REPORT	b. ABSTRACT	c. THIS PAGE	17. LIMITATION OF ABSTRACT	18. NUMBER OF PAGES	19a. NAME OF RESPONSIBLE PERSON
U	U	U	UU	27	HQ - STI-infodesk@mail.nasa.gov
					19b. TELEPHONE NUMBER *(Include area code)* 757-864-9658